OPTIMIZATION OF TWO-DIMENSIONAL WING IN GROUND EFFECT CONSIDERING AERODYNAMIC CENTER OF HEIGHT AND LIFT

Juhee Lee*, Sungjun Joo**
***Hoseo University, **EeGen**
juheelee@hoseo.eud;drjoo@eegen.com

Keywords: *Aerodynamic characteristics; CFD (Computational Fluid Dyamics); WIG (Wing-in-ground) effect vehicle; Pareto set; Aerodynamic center of height list*

Abstract

The Numerical optimizations of a 2-dimensional wing in ground effect considering aerodynamic characteristics and aerodynamic center of height have been performed and Pareto optima (potential solutions) have been closely investigated. Due to the ground effect (reducing induced drag and increasing lift), it is expected that a WIG effect vehicle shows high operational efficiency. However, in terms of the trade-off between the aerodynamic forces and the stability, the WIG effect vehicle scarifies its efficiency to meet the stability somewhat. In this study, the lift coefficient, the lift–drag ratio and the aerodynamic center of height are chosen as the objective functions to obtain the optimal wing profiles for the WIG effect vehicle. The optimal solutions of the multi-objective optimization are not unique but a set of the non-dominated optima: the Pareto frontiers or a Pareto set. As the results of the multi-objective optimization, the one hundred fourteen of Pareto optima that include high-lift, high efficiency, and more stable airfoils on the edge of the 3-dimensional objective space, are obtained at thirty evolutions.

1 Introduction

The wing-in-ground (WIG) effect vehicle is an advanced vehicle that cruises close to water or ground surface (i.e., at a height of 30% of its chord length or lower) by utilizing an air cushion among the wing, the fuselage and the ground. Due to the air cushion at low heights, there is a considerable increase in lift and a decrease in drag and therefore enhancement of the lift–drag ratio. Neither the speed of a fast ship nor the efficiency of an economical aircraft can be better than that of the WIG effect vehicle. However, there are a few technical difficulties in cramping the progress of the potential WIG effect vehicle; hump drag [1], static height stability [2] and so on.

Kornev and Matveev [3] performed an analysis of the static height stability using vortex lattice methods (VLM). In their study, there were three important factors for static height stability: tail unit, profiles of wing sections, and main wing pro-file. The static height stability for the WIG effect vehicle could not be satisfied by moving the center of gravity. The favorable range of the height stability for the stable flight in ground effect was between -0.15 and -0.05. For the stable flight, they insisted that the center of gravity should be located between the aerodynamic centers of altitude and pitch and, furthermore, the close location to the center of altitude was favorable.

Im and Chang [4] investigated the aerodynamic characteristics of a cambered airfoil, NACA4415, under the free-flight conditions of M = 0.5, 2, 4 and h = 0.15, 0.3, 0.5. They showed that the lift-to-drag ratio of NACA4415 is slightly increased as the vehicle is approaching to the ground. They also found that the pressure is increased at the leading edge only for the case of small angle of attack (α). Recently, Park and Lee [5] carried out a numerical investigation into the effect of an endplate at various angle attacks and ground

clearances. They found that the endplate preventing the high-pressure air escaping from the lower wing surface reduced the influence of wing-tip vortex and augmented lift and lift-drag ratio further. The endplate also reduced the deviation of the static height stability with respect to pitch angles and heights. However, the comparison of Irodov's stability criteria [6] showed that the endplate was not favorable for static height stability.

Optimal design of the WIG airfoil was studied by only a few researchers. Most of them treated the single objective optimization with the local optimization technique. Kim and Chun [7] performed the computational optimization for airfoil shape. They chose the pressure distributions (inverse design) and lift coefficient as the objective functions and obtained the optimal solutions by using a sequential quadratic programming (SQP) method which is one of the gradient-based local optimization technologies. However, it is hard to find researches on the airfoil shape optimization of WIG craft considering multilateral design objectives.

For designing a WIG effect vehicle with high cruise performance, it is difficult to satisfy the design requirements such as efficiency and stability, simultaneously, because of the trade-off phenomena between them. Park and Lee [1] per-formed a multi-objective optimization for the 2-dimensional WIG effect vehicle by integrating CFD and MOGA (multi-objective genetic algorithm).

In this study, in order to obtain stable and high-performance airfoils under the influence of ground effect, the shape optimization with genetic algorithm (GA) is performed numerically. The lift coefficient, lift-to-drag ratio and aerodynamic center of height (X_h), which significantly influence the performance of the WIG craft, are adopted as the objective functions. The airfoil shape is parameterized by Bezier curves and their control points are used as the design variables. The non-dominated optimal solutions, known as the Pareto frontier (or sets), can be obtained by using a multi-objective genetic algorithm (MOGA). Due to the trade-offs between the conflicting objective functions, the optimal solutions become a number of the individuals (i.e., designs), which are not dominated by the other individuals within the design space.

2 Computational Model and Optimization

2.1 Governing Equation

The flow around an airfoil is assumed to be two-dimensional, turbulent and steady state with incompressible fluid. The turbulent flow of air is described by the Reynolds-Averaged Navier-Stokes (RANS) equations and it can be ex-pressed in tensor notation for mass and momentum as follows:

$$\frac{\partial}{\partial x_j}\left(\rho u_j\right)=0 \tag{1}$$

$$\frac{\partial}{\partial x_j}\left(\rho u_j u_i-\tau_{ij}\right)=-\frac{\partial p}{\partial x_i} \tag{2}$$

$$\tau_{ij}=\mu_t S_{ij}-\frac{2}{3}\mu_t\frac{\partial u_k}{\partial x_k}\delta_{ij}-\rho\overline{u_i' u_j'} \tag{3}$$

where x_i , j =1, 2 are the Cartesian coordinate vector, u_i are the mean velocity components. $-\rho\overline{u_j' u_i'}$ is the Reynolds stress tensor. μ_t and s_{ij} are the turbulent viscosity and the modulus of the mean strain rate tensor, respectively, which are defined as

$$\mu_t=f_t\cdot C_t\frac{\rho k^2}{\varepsilon},\ S_{ij}=\left(\frac{\partial u_i}{\partial x_j}+\frac{\partial u_j}{\partial x_i}\right) \tag{4}$$

In the present study, the RNG $k-\varepsilon$ model proposed by Yakhot et al. [8] is applied to model the turbulent flow around the airfoil. It is known that the RNG $k-\varepsilon$ model included an additional term in the ε -equation can significantly improve the accuracy for airfoil flows.

2.2 Validation of CFD Models

Air is taken as the working fluid and is assumed to be steady, incompressible, and turbulent flow.

The fluid proper-ties are taken to be constant and the effect of viscous dissipation is assumed to be negligibly small. The numerical simulations presented in this work were done by means of STAR-CD [9] which is a general purpose commercial software. For representing the exact flight conditions, the moving wall boundary condition with a flight velocity is applied at the ground.

The solutions are treated as converged ones when the sum of normalized residual is less than 1×10^{-7}. In order to check the grid dependency and to verify the CFD models and the evaluation processes, the aerodynamic forces of the NACA0015 airfoil are compared with the experimental results [5] as shown in Fig. 1. The C_l as a function of a and drag polar for the two Reynolds numbers ($\mathrm{Re}=1.27\times10^6$ and 3.26×10^6) are calculated and they are compared with those of the experiment, which were conducted by Jacobs and Sherman [10]. The three consecutive numbers of meshes, around 11,000 (coarse), 17,000 (base) and 24,000 (refined), are used to test the grid dependency and the results are presented. The computational domain used in this study is ex-tended 10 times of the chord for each direction to avoid the influence of the far boundaries but is extended 20 times for the downstream direction. The upstream boundary is modeled using a velocity inlet boundary condition with a uniform velocity distribution. The downstream boundary is modeled using a pressure-outlet boundary condition. A slip-wall boundary condition is imposed on the undisturbed far boundary, thereby imposing a zero cross-flow condition. The airfoil surface modeled as solid walls with a no-slip boundary condition enforced. To predict the boundary flow on the airfoil surface properly, the non-uniformly distributed h-type grid, which is dense in the vicinity of the airfoil surface, is used. The grid system and the computational domain are same except for the ground. It is found in Fig. 1 that and the drag polar are overestimated for the coarse grid compared with the experiment, while those for the base and refined grid are estimated properly. In order to save computational time, the base grid is employed in this study.

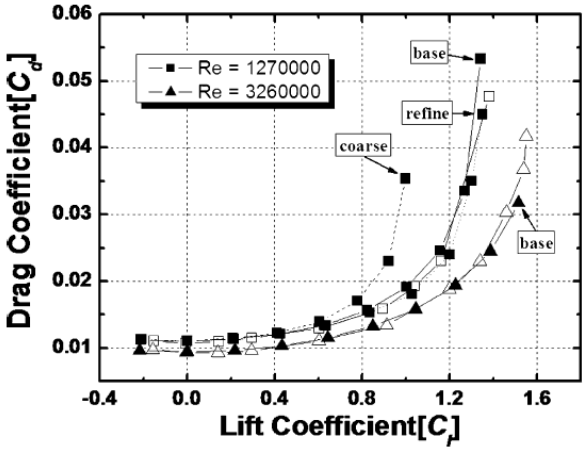

Fig. 1 Comparison of aerodynamic forces: drag polar for two Reynolds numbers (hollow: experiments (Jacobs and Sherman, 1937); filled: present study).

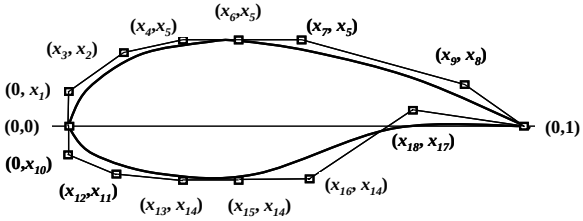

Fig. 2 Airfoil geometry parameterization.

A schematic configuration and a coordinate system of air-foils in WIG craft considered in this study are shown in Fig. 2.

2.3 Optimization

Twenty-five individuals for one population are used and the selection pressure is adopted so as to enhance the convergence rate. In each tournament, two candidates are randomly selected from the current generation, and through two competitions, the winner has a chance to become a parent for reproduction. The number of cutting lines used for exchanging genes for the crossover operation is important. In this study, two cutting lines are used to maximize the life of the schema, which is a useful pattern in the gene. Mutation is the occasional random alteration of the value of a string with a small probability. When the value of mutation is about a few percent, the GA cannot converge to proper solutions with the evolutions and becomes a completely random search. To prevent the operation from becoming a random search and keep the balance between exploitation and exploration, a 0.5% mutation rate is chosen. On the other hand, when a new

offspring individual is found to be a genetic twin in the next generation, that individual is ignored, and one more individual will be generated.

The formulation of the optimization is as follows;

$$\text{Find control points} \quad X = \{x_1, x_2, \cdots, x_{18}\}^T \tag{5}$$

$$\text{To maximize} \quad F_1(x) = C_l \tag{6}$$

$$\text{To minimize} \quad F_2 = |X_h| = |C_{m,h} / C_{l,h}| \text{ at } x = ac \tag{7}$$

$$\text{To maximize} \quad F_3 = C_l / C_d \tag{8}$$

The aerodynamic center of height is employed as one of objectives instead of stability which consists of two aerodynamic centers of pitch and height. The aerodynamic center of pitch is mainly controlled by a horizontal tail. If the X_h is placed next to the quarter-chord, the strict stability condition, $X_h \le X_{cg} < X_a$ and $X_h \sim X_{ac}$, can be easily satisfied by horizontal tail and reduce the area of the horizontal tail.

3 Results and Disccussion

3.1 Pareto Set

SMOGA (simple multi-objective genetic algorithm) developed by authors and based on the GA is different from the random search but cannot obtain exactly same Pareto set every performance because of its random work in mutation operations and selection operation. To confirm computational feasibility of SMOGA, the optimization is performed three times in a raw. The three Pareto set obtained are plotted in Fig. 3. Approximately 100 potential solutions (Pareto individuals) can be obtained each performance. To observe the tendency of the Pareto set, only one-fourth individuals are plotted in Fig. 3. The lines in Fig. 3 are linear regression. Every try has a little deviation but they show similar tendency and all Pareto

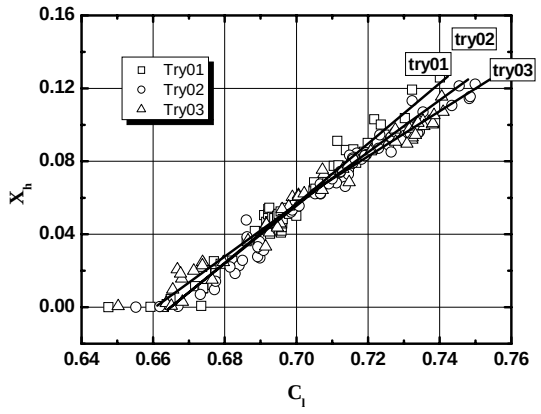

Fig. 3 Comparison of Pareto set from three optimizations.

individuals are placed in a small band. As a result, SMOGA used in this study can find Pareto optima properly without any weighing functions that a value of the function is cumbersome problem for a single-objective optimization.

Genetic algorithm is a heuristic process and the average fitness of all the individuals in a generation is gradually improved as the evolution. Fig. 4 shows the on- and offline performance according to the generation, in order to examine the convergence histories for lift, aerodynamic center of height and lift-drag ratio. DeJong [11] devised two performance measures (i.e., online and offline) to quantitatively evaluate the performance of the GAs and they are defined as follows,

Abbreviations should be spelt out in full the first time they appear and their abbreviated form included in brackets immediately after. Words used in a special context should appear between single quotation marks the first time they appear.

$$f_e^{on-line}(i) = \frac{1}{i}\sum_{j=1}^{i} f_e(j) \tag{9}$$

$$f_e^{off-line}(i) = \frac{1}{i}\sum_{j=1}^{i} f_e^*(j) \tag{10}$$

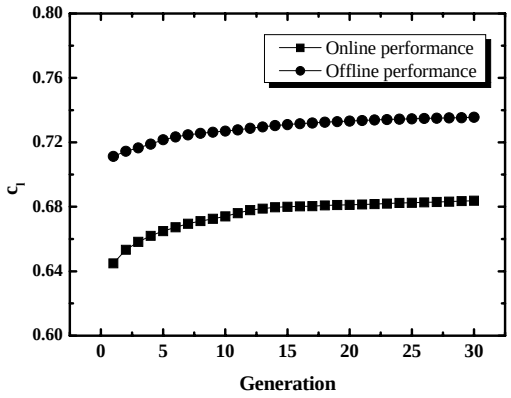

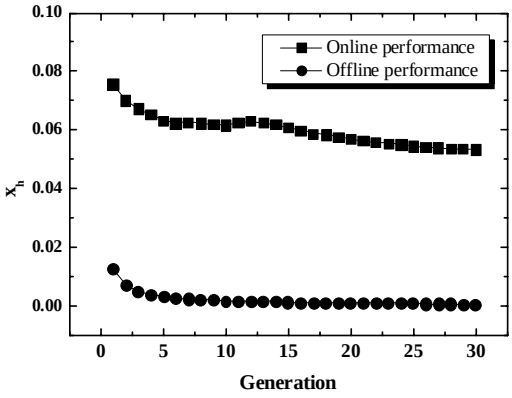

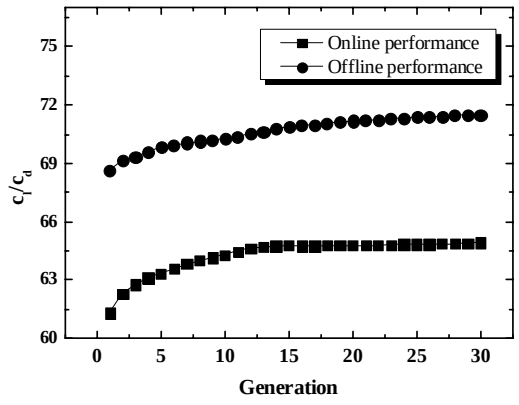

Fig. 4 On- and offline-performance for convergence history.

Where $f_e(j)$ is the value of objective functions at generation i for environment e, $f_e^*(j)$ the best value of objective functions until a given generation i for $j = 1,2,...,i$. The online performance, $f_e^{on-line}(i)$, is an average fitness of all trials up to the current generation and the

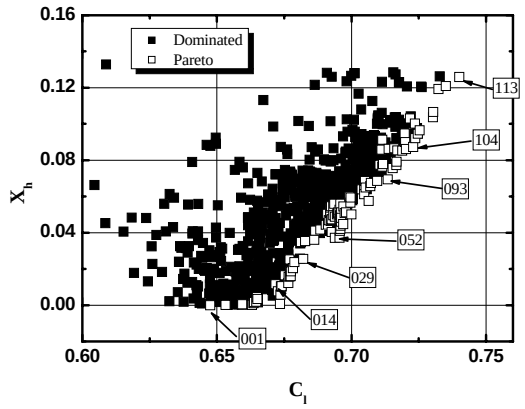

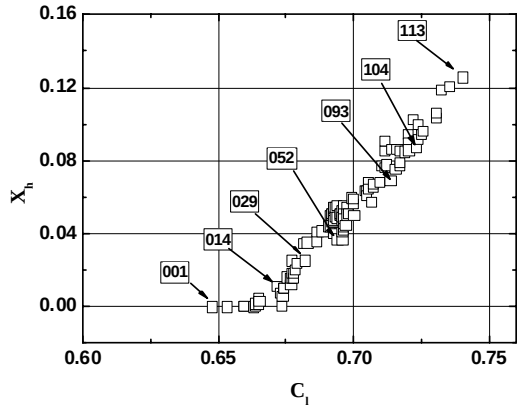

Fig. 5 Pareto set and dominated individuals with respect to C_l and X_h .

offline, $f_e^{off-line}(i)$, is a running average of the best individuals up to a particular generation. In addition, the online performance is used to measure the developing performance while the offline one is originally devised to gauge the convergence of optimization process for the single objective optimization problem. As shown in Fig. 4, the objective functions are gradually converged as the generation is advanced. It can be seen that a moderate convergence is achieved for all of objective functions after 20~25 generations are proceeded.

Pareto individuals are numbered according to their lift coefficient from 1 (the lowest lift coefficient) to 114 (the highest lift coefficient) in Fig. 5. In order to observe effects between profile and objectives, seven individuals are randomly selected among Pareto set as shown in Fig. 5. A multi-objective optimization does not

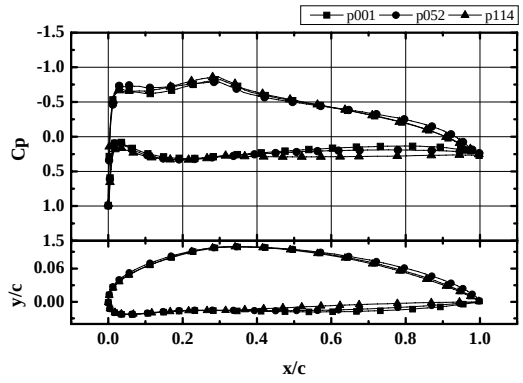

Fig. 6 Comparison of C_p and airfoil profile; p001, p052 and p114.

look for a unique solution but a set of them. From the Pareto frontier point of view, none of the optima are dominated. This implies that none of the objectives can be improved without the worsening of at least one of the other objectives. The tradeoff between objectives (lift coefficient and X_h) can be observed in Fig. 5.

When the lift is improved, the X_h is degraded and vice versa. The actual values of X_h are negative (-), and thus locations of the aerodynamic center of height are downstream of a quarter-chord. It lead difficulty of designing WIG vehicle because of it aerodynamic center of pitch angle should be downstream of X_h. It implies that the WIG vehicle should equip a large horizontal tail and sophistic control to sustain its stabile condition when it cruises in ground effect.

3.2 Characteristics of Pareto Set

In order to compare aerodynamic characteristics and stabil-ity, the profile and its pressure distribution along the surface are plotted in Fig. 6. According to profile's characteristics, difference in upper and lower surface around trailing edge can be observed. The straight lower surface in Fig. 6 can utilize the ground effect and minimize the Venturi effect which en-forces negative lift force locally. In this study, the thickness of p114 (high lift) is thick while thickness of p001 (high X_h) shows straight lower surface which improves lift further. In case of the p001, distance between lower surface and ground is decreased until minimum point around $x/c = 0.75$. After the minimum point, the distance increase slightly and thus, it implies diverge-converge passage next to the trailing edge. This diverge-converge passage might reduce the lift but X_h might be improved. The passage reduces the C_m at a quarter-chord as well as deviation of the C_m with respect to heights. The pressure distribution on the lower surface will be in-creased with decreasing distance between ground and airfoil. At the same time the Venturi effect will increase. Consequently, the moment coefficient with respect to aerodynamic center will slight increase or sustain. These phenomena can improve X_h.

The negative $C_{l,h}$ implies that the vehicle cannot sustain its flight height when it meets a small disturbance and be-comes unstable. Therefore, the operation in the angle of attack is not acceptable and is excluded from analysis. Considering airfoil only used in this study, the values of X_h can be whether it is negative or positive. More important factor for helping successful design of WIG vehicle is the location of the X_h. That is, the location of the is as close to AC (aero-dynamic center) as possible and sufficient stability margin ($X_h - X_\alpha$) can be obtained consequently and center of gravity (CG) is conveniently located between X_h and X_α; which is a strict condition for static height stability [12]. As shown in Fig. 7, the locations of X_h according to angles of attack (α) move backward along the down stream of the AC. X_hs for three Pareto individuals are located at 25% downstream from AC (a quarter chord) and the location of the X_h from the leading edge therefore is about 50%. CG should be located behind 50% of a chord and the stability margin is reduced also. To compensate the reduced stability margin and satisfy the static height stability ($X_h - X_\alpha$), it is require the large horizontal tail at high angle of attack such as $\alpha = 10$. It should be avoid such a high angle of

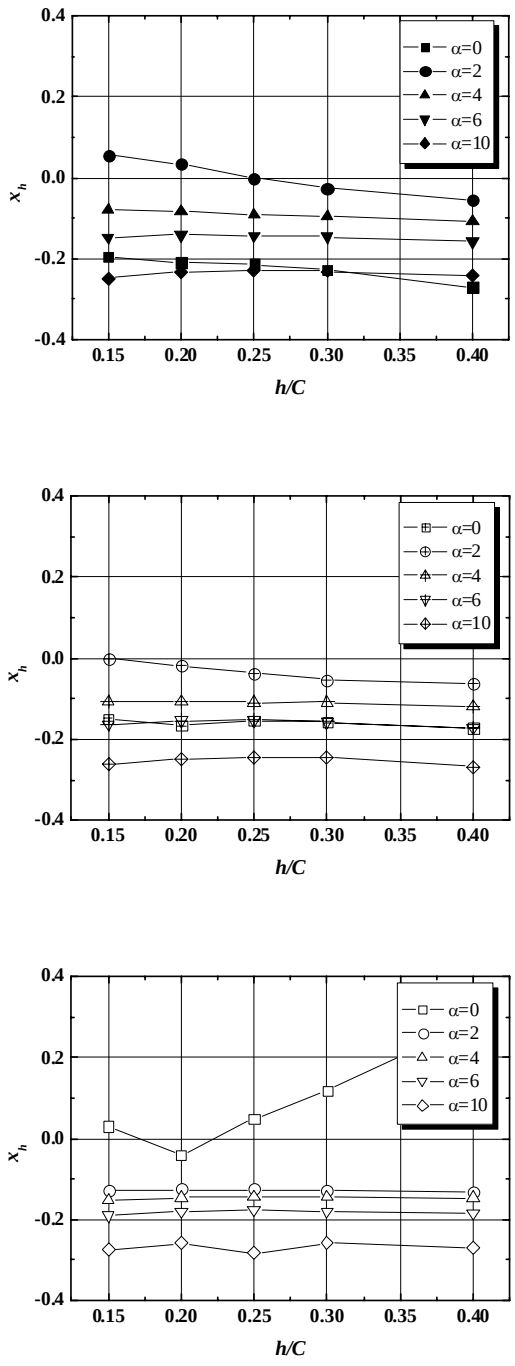

Fig. 7 Stability of Pareto individuals: p001, p052 and p114.

attack when the vehicle is in ground effect. Except this angle of attack of 10, the X_h is bounded within 0.15 as shown in Fig. 7. X_h s of both p001 and p052 become similar. The optimization is performed at $\alpha = 2$ and $h/c = 0.25$ and therefore, the smallest absolute value of can be observed for three cases. s of p001 and p052 move upstream as the decreasing height whereas X_h for p114 is stationary. X_h for p001 and p052 slightly move forward and 6 that X_h for p114 is constant for $\alpha = 4$ and 6 as the height changes for three cases. From Fig. 7, p001 and p052 which have a s-shape lower surface show upstream location of X_h (stable) than that of p114 which has straight lower surface and show the highest lift coefficient.

4 Conclusions

The shape optimization of a 2-dimensional airfoil under ground effect has been carried out by the integration of CFD (computational fluid dynamics) and MOGA (multi-objective genetic algorithm). From the analysis of these Pareto optima, which include the various airfoil shapes, it was found that the relation between C_l and C_l / C_d is linearly dependent but the other two relationships, between X_h and C_l and between X_h and C_l / C_d, are not. The airfoil profiles of the lower side become flat for the high lift individuals and diverge-converge shape next to the trailing edge for the favorable X_h. This flat airfoil can prevent the Venturi effect and improves the ram effect further. This flat shape helps to reduce the drag and increase the lift simultaneously. On the other hand, the Venturi effect improves the X_h by decreasing moment coefficient with respect to height and deviation of the moment. In near future, we are going to build a WIG effect vehicle whose wing section is one of the Pareto individual. The static height stability ($X_h - X_\alpha$) of a WIG effect vehicle which has all compartments such as main wing, horizontal wing and fuselage will be closely investigated.

References

[1] K.W. Park and J.H. Lee, Optimal design of two-dimensional wings in ground effect using multi-objective genetic algorithm, *Ocean Engineering*, Vol. 37, pp. 902-912, 2010.

[2] K.V. Rozhdestvensky, Wing-in-Gground Effect Vehicles, *Progress in Aerospace Sciences*, Vol. 42, pp. 211-283, 2006.
[3] N. Kornev and K. Matveev, *Complex numerical modeling of dynamics and crashes of wing-in-ground vehicles*, AIAA 2003-600, 2003.
[4] Im, Y.H., Chang, K.S., Flow Analysis of a Three-Dimensional Airfoil in Ground Effect, *Journal of the Korean Society for Aeronautical and Space Sciences* , Vol. 29, No. 5, pp. 1-8, 2000. (in Korean)
[5] Park, K.W., Lee, J.H., Influence of endplate on aerodynamic characteristics of low-aspect-ratio wing in ground effect, *Journal of Mechanical Science and Technology*, Vol. 22, pp. 2578-2589, 2008.
[6] Irodov, R.D., Criteria of longitudinal stability of Ekranoplan, *Ucheniye Zapiski TSAGI*, Vol. 1, No. 4 Moscow 1970.
[7] Kim H.J., Chun H.H., Design of 2-Dimensional WIG Section by a Nonlinear Optimization Method, *Journal of the Society of Naval Architects of Korea* , Vol. 35, No. 3, pp. 50-59, 1998.
[8] Yakhot, V., Orszag, S.A., Thangam, S., Gatski TB, Spezoale CG, Development of Turbulent Models for Shear Flows by a Double Expansion Technique, *Physics Fluids*, Vol. 4, No. 7, pp. 1510-1520, 1992.
[9] STAR-CD+ v4.02, *Methodology*, Computational Dynamics, Co., London. U. K, 2002.
[10] E.N. Jacobs and A. Sherman, *Airfoil Section Characteristics as Affected by Variations of the Reynolds Number*, NACA TM586, 1939.
[11] DeJong KA, *An Analysis of the Behavior of a Class of Ge-netic Adaptive Systems*, Doctoral Thesis, Department of Computer and Communication Sciences University of Michigan, Ann Arbor, 1975.
[12] Kornev, N., and Matveev, K., *Complex Numerical Modeling of Dynamics and Crashes of Wing-in-ground vehicles*, AIAA 2003-600, 2003.

Copyright Statement